Hybrid lipid self-assembling nanoparticles for brain delivery of microRNA

Virginia Campani[a], Silvia Zappavigna[b], Lorena Scotti[a], Marianna Abate[b], Manuela Porru[c], Carlo Leonetti[c], Michele Caraglia[b,d], Giuseppe De Rosa[a,*]

[a] Department of Pharmacy, University Federico II of Naples, Via Domenico Montesano, 49, 80131 Naples, Italy
[b] Department of Precision Medicine, University of Campania "Luigi Vanvitelli", Via Santa Maria di Costantinopoli, 16, 80138 Naples, Italy
[c] Department of Research, Advanced Diagnostic, and Technological Innovation, IRCCS Regina Elena National Cancer Institute, Via Elio Chianesi, 53, 00144 Rome, Italy
[d] Biogem Scarl, Institute of Genetic Research, Laboratory of Molecular and Precision Oncology, 83031 Ariano Irpino, Italy

ARTICLE INFO

ABSTRACT

Hybrid self-assembling nanoparticles (SANPs) have been previously designed as novel drug delivery system that overcomes stability issues following long-term storage and with an easy scale-up. This system has been successfully used to deliver anionic-charged agents, e.g. bisphosphonates, in different types of tumors, such glioblastoma (GBM). Here, SANPs were tested and optimized for the delivery of nucleic acids, in particular of a specific microRNA, e.g. miR603, used for its potential role in controlling the chemoresistance in different forms of cancer, e.g. (GBM).

To this aim, SANPs with different lipids were prepared and characterized, in terms of size, polydispersity index, zeta potential, miRNA encapsulation, stability in BSA, serum and hemolytic activity. Then, SANPs were tested in vitro on two different cell lines of GBM. Finally, miRNA biodistribution was tested in vivo in an orthotopic model of GBM.

The majority of the formulations showed good technological characteristics and were stable in BSA and serum with a low hemolytic activity. The intracellular uptake studies on GBM cell lines showed that SANPs allow to achieve a higher miRNA delivery compared to others transfection agents, e.g. lipofectamine. Finally, in vivo biodistribution studies in an orthotopic of GBM demonstrated that the optimized SANP formulations, were able to deliver miRNA in different organs, e.g. the brain.

1. Introduction

Lipid nanocarriers have been largely proposed to overcome the biopharmaceutical issues associated with the therapeutic use of non-coding RNAs (nc-RNAs) (Campani et al., 2016). The efficacy of this strategy is confirmed by current ongoing clinical trials using lipid nanoparticles to deliver ncRNAs in different forms of cancer (Kanasty et al., 2013; Xu et al., 2015) and with the recent approval of the first RNA-based therapy (ONPATTRO®). However, despite the significant efforts in the field of nanomedicine, the number products approved or in advanced stage of clinical trial remains very limited, especially for the delivery of nucleic acids. In addition, while the use of nanomedicine for the delivery of nucleic acids into the liver is not an issue, extrahepatic delivery in sites such as the brain remains a challenge. The clinical development of nanomedicine is the hampered by different issues, among them instability following long-term storage and the difficult scale-up (Etheridge et al., 2013). Our group recently developed and patented lipid hybrid self-assembling nanoparticles (SANPs) for the delivery of bisphosphonates in the tumors (Salzano et al., 2011; Marra et al., 2012; Salzano et al., 2016). This formulation has been developed by combining PEGylated cationic liposomes and calcium/phosphate nanoparticles. Cationic liposomes are able to complex RNA promoting its delivery into the cells; PEGylation should assure long circulation into the blood; calcium/phosphate nanoparticles are known as transfection agent able to promote the endosomal escape (Li et al., 2010). This formulation has been designed to accelerate the scale-up process and to avoid issues due to the physical instability following long-term storage. Indeed, the nanoparticles are prepared before use by a self-assembling process starting from components easily prepared in pharmaceutical grade. These nanoparticles have been successfully used to deliver bisphosphonates in brain tumours (Salzano et al., 2016; Porru et al., 2014).

Here, we investigated the possibility to use SANPs for ncRNA delivery, e.g. microRNA (miRNA). Due the ability to deliver bisphosphonates in the central nervous system (CNS), SANPs have been tested

for their ability to deliver miRNA in an experimental model of brain tumor. Among the primary brain tumors, glioblastoma (GBM) is the highest aggressive one with very poor prognosis (about 14.6 months) (Stupp et al., 2009). GBM is currently treated with radiotherapy in combination with chemotherapy, namely temozolomide (TMZ). However, TMZ, especially after prolonged treatments, has only a very limited activity mainly due to the occurrence of chemoresistance mainly attributed to the activity of the O^6-methylguanine methyl transferase (MGMT) (Pegg, 1990; Ochs and Kaina, 2000; Perazzoli et al., 2015). Recently, a microRNA (miRNA), namely miRNA-603, has been identified as powerful suppressor of MGMT expression in GBM (Kushwaha et al., 2014). These findings suggest the possibility to use miRNAs as powerful tool to enhance the efficacy on DNA alkylating agent, e.g. TMZ, in the treatment of GBM.

The aim of this study was to propose and optimize SANPs for the delivery of miRNA in brain tumor. To this aim, SANPs with different lipid composition, i.e. different cationic lipids, neutral lipids, and type of PEGylated lipids, have been tested. All the prepared SANPs were characterized in terms of size, zeta potential and miRNA encapsulation. Stability of SANPs have been tested in bovine serum albumin (BSA) or plasma; moreover, hemolytic activity of the formulations on red blood cells was investigated. Cytotoxicity of the different prepared SANPs was also tested on two different GBM cell lines. Then, formulations selected in the previous studies were tested for the delivery of the miR603 in two GBM cells. Finally, the biodistribution of the miRNA, when administered with SANPs was studied in different organs in an orthotopic model of GBM.

The SANP composition, in terms of cationic lipids, presence of neutral lipids, and type of PEGylated lipids, was optimized to achieve the highest delivery of the miRNA. Thus, three different cationic lipids, namely 1,2-dioleoyl-3-trimethylammonium-propane chloride (DOTAP), N-[1-(2,3-dioleyloxy)propyl]-N,N,N-trimethylammonium chloride (DOTMA) or 3ß-[N-(N',N'-dimethylaminoethane)-carbamoyl]cholesterol hydrochloride (DC-chol), two neutral lipids, namely cholesterol (CHOL) and dioleoylphosphatidylethanolamine (DOPE), and two PEGylated lipids, namely N-palmitoyl-sphingosine-1 {succinyl [methoxy(polyethylene glycol)$_{2000}$]} (PEG$_{2000}$-Cer[16]) (cer-PEG) and 1,2-distearoyl-sn-glycero-3-phosphoethanolamine-N-[amino(polyethylene glycol)-$_{2000}$] (DSPE-PEG$_{2000}$) were tested in this study.

2. Material and methods

2.1. Material

MicroRNA (miRNA), namely microRNA-603 (miR603) (5′-CACAC ACUGCAAUUACUUUUGC-3′), was synthesized by Tema Ricerca s.r.l. (Bologna, Italy). 1,2-dioleoyl-3-trimethylammonium-propane chloride (LIPOID DOTAP-CL or DOTAP) was kindly gifted by Lipoid GmbH (Ludwigshafen, Germany), N-[1-(2,3-dioleyloxy)propyl]-N,N,N-trimethylammonium chloride (DOTMA) or 3ß-[N-(N',N'-dimethylaminoethane)-carbamoyl]cholesterol hydrochloride (DC-chol), cholesterol (CHOL), dioleoylphosphatidylethanolamine (DOPE), N-palmitoyl-sphingosine-1 {succinyl[methoxy(polyethylene glycol)$_{2000}$]} (cer-PEG$_{2000}$) (cer-PEG) and 1,2-distearoyl-sn-glycero-3-phosphoethanolamine-N-[amino(polyethylene glycol)-$_{2000}$] (DSPE-PEG$_{2000}$) were from Avanti Polar Lipids (Alabaster ,a Usa). Sodium chloride, calcium chloride, sodium phosphate dibasic, potassium chloride and bovine serum albumin (BSA), were obtained from Sigma-Aldrich Co. (Milan, Italy). Human plasma was obtained from healthy volunteers.

2.2. Methods

2.2.1. Preparation of hybrid self-assembling nanoparticles encapsulating miRNA (SANPs-miRNA)

Hybrid self-assembling nanoparticles (SANPs) were prepared as previously reported (Salzano et al., 2011) with some modifications. In a first step, PEGylated cationic liposomes (PLs) consisting of DOTAP/chol/DSPE-

PEG$_{2000}$ (mM ratio 1:1.8:0.125), DOTAP/DSPE-PEG$_{2000}$ (mM ratio 1:0.125), DOTAP/DOPE/DSPE-PEG$_{2000}$ (mM ratio 1:1:0.125), DOTMA/chol/DSPE-PEG$_{2000}$ (mM ratio 1:1.8:0.125), DOTMA/DSPE-PEG$_{2000}$ (mM ratio 1:0.125), DOTMA/DOPE/DSPE-PEG$_{2000}$ (mM ratio 1:1:0.125), DC-chol/chol/DSPE-PEG$_{2000}$ (mM ratio 1:1.8:0.125), DC-chol/DSPE-PEG$_{2000}$ (mM ratio 1:0.125), DC-chol/DOPE/DSPE-PEG$_{2000}$ (mM ratio 1:1:0.125), DOTAP/chol/cer-PEG (mM ratio 1:1.8:0.125), DOTAP/cer-PEG (mM ratio 1:0.125), DOTAP/DOPE/cer-PEG (mM ratio 1:1:0.125), DOTMA/chol/cer-PEG (mM ratio 1:1.8:0.125), DOTMA/cer-PEG (mM ratio 1:0.125), DOTMA/DOPE/cer-PEG (mM ratio 1:1:0.125), DC-chol/chol/cer-PEG (mM ratio 1:1.8:0.125), DC-chol/cer-PEG (mM ratio 1:0.125), DC-chol/DOPE/cer-PEG (mM ratio 1:1:0.125) were prepared by hydration of a thin lipid film followed by extrusion. Briefly, the thin film was obtained by a rotary evaporator (Laborota 4010 digital, Heidolph, Schwabach, Germany) and then hydrated with RNAse free water for 2 h. The liposome suspension was then extruded using a thermobarrel extruder system (Northern Lipids Inc., Vancouver, BC, Canada) passing repeatedly the suspension under nitrogen through polycarbonate membranes with decreasing pore sizes from 400 to 100 nm (Nucleopore Track Membrane 25 mm, Whatman, Brentford, UK). After preparation, liposomes were stored at 4 °C. Separately, calcium-phosphate colloidal dispersion (CaP NPs) were prepared. Briefly, an aqueous solution of dibasic hydrogen phosphate (10.8 mM) at pH 9.5 was added 1:1 v/v, dropwise and under magnetic stirring at about 1500 rpm, to an aqueous solution of calcium chloride (18 mM) at pH 9.5 for 10 min and filtered with cellulose filter (0.22 μm filter membranes of regenerate cellulose). CaP NPs were prepared before the use. The colloidal dispersion was then mixed with an aqueous solution of miRNA (0.2 mM of miRNA in RNAse free water corresponding to 1.4 mg/ml of miR603) by vortex for 10 s in a ratio of 50:1 v/v and allowed to react for 10 min, resulting in CaP/miRNA NPs. Finally, SANPs-miRNA (Fig. 1), were prepared by mixing, in equal volume, CaP/miRNA NPs and different PLs by vortex for 10 s and allowed to react for 25 min. The concentration of miR603 in the final formulations was 35 μg/ml. Plain SANPs, without miRNA, were prepared similarly. Each formulation was prepared in triplicate.

2.2.2. Physical-chemical characterisation of self-assembling nanoparticles encapsulating miRNA (SANPs-miRNA) and plain SANPs

PLs, plain SANPs (without miRNA) and SANPs-miRNA were characterized in terms of mean diameter, polydispersity index (PI), and zeta
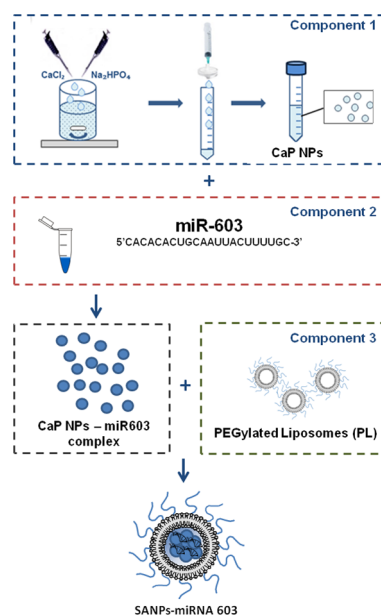

Fig. 1. Preparation of hybrid self-assembling NPs encapsulating miRNAs (SANPs-miRNA). CaP NPs = calcium phosphate nanoparticles.

Table 1
Composition of the different formulations of hybrid self-assembling nanoparticles (SANPs) prepared plain or complexed with miR603.

Lipid composition of the formulation (mM ratio)							Formulation legend		
DOTAP	DOTMA	Dc-Chol	CHOL	DOPE	DSPE-PEG	cer-PEG	Cationic liposome	SANPs	SANPs encapsulating miR603
1	–	–	1.8	–	0.125	–	PL-DOTAP C1	SANPs-DOTAP C1	SANPs-603-DOTAP C1
1	–	–	–	–	0.125	–	PL-DOTAP 1	SANPs-DOTAP 1	SANPs-603-DOTAP 1
1	–	–	–	1	0.125	–	PL-DOTAP D1	SANPs-DOTAP D1	SANPs-603-DOTAP D1
–	1	–	1.8	–	0.125	–	PL-DOTMA C1	SANPs-Dotma C1	SANPs-603-Dotma C1
–	1	–	–	–	0.125	–	PL-DOTMA 1	SANPs-Dotma 1	SANPs-603-Dotma 1
–	1	–	–	1	0.125	–	PL-DOTMA D1	SANPs-Dotma D1	SANPs-603-Dotma D1
–	–	1	1.8	–	0.125	–	PL-Dcchol C1	SANPs-Dcchol C1	SANPs-603-Dcchol C1
–	–	1	–	–	0.125	–	PL-Dcchol 1	SANPs-Dcchol 1	SANPs-603-Dcchol 1
–	–	1	–	1	0.125	–	PL-DCchol D1	SANPs-Dcchol D1	SANPs-603-Dcchol D1
1	–	–	1.8	–	–	0.125	PL-DOTAP C2	SANPs-DOTAP C2	SANPs-603-DOTAP C2
1	–	–	–	–	–	0.125	PL-DOTAP 2	SANPs-DOTAP 2	SANPs-603-DOTAP 2
1	–	–	–	1	–	0.125	PL-DOTAP D2	SANPs-DOTAP D2	SANPs-603-DOTAP D2
–	1	–	1.8	–	–	0.125	PL-DOTMA C2	SANPs-DOTMA C2	SANPs-603-DOTMA C2
–	1	–	–	–	–	0.125	PL-DOTMA 2	SANPs-DOTMA 2	SANPs-603-DOTMA 2
–	1	–	–	1	–	0.125	PL-DOTMA D2	SANPs-DOTMA D2	SANPs-603-DOTMA D2
–	–	1	1.8	–	–	0.125	PL-DCchol C2	SANPs-DCchol C2	SANPs-603-DCchol C2
–	–	1	–	–	–	0.125	PL-DCchol 2	SANPs-DCchol 2	SANPs-603-DCchol 2
–	–	1	–	1	–	0.125	PL-DCchol D2	SANPs-DCchol D2	SANPs-603-DCchol D2

potential (ζ). In particular, mean diameter was determined at 20 °C by photon correlation spectroscopy (PCS) (N5, Beckman Coulter, Miami, USA) while zeta potential (ζ) was measured in deionized and filtered water by the Zetasizer Nano Z (Malvern, UK). For each formulation, the mean diameter, the PI and the ζ were calculated as the mean of measures carried out on at least three different batches.

2.2.3. miRNA encapsulation into SANPs

Moreover, in the case of SANPs-miRNA, the miRNA encapsulation efficiency was also determined in the different formulations. Briefly, the amount of miR603 encapsulated in the final SANPs-miRNA was determined by indirect measure of unencapsulated miRNA, separated by ultracentrifugation (Optima Max E, Beckman Coulter, USA) at 80000 rpm, 4 °C, for 40 min. The supernatants were analyzed by UV (UV-1800, UV Spectrophotometer) at the wavelengths of 260 nm and the concentration of miRNA was calculated by a calibration curve of miR603 ($R^2 = 0,999$) in H_2O. Each analysis was carried out in duplicate.

2.2.4. Stability of SANP-miRNA in biological media

The stability of SANPs and SANPs-miRNA was tested in bovine serum albumin (BSA), (1% w/v in 20 mM phosphate buffer saline, isosmotic with NaCl 0,9% w/v physiological solution)) and human plasma. To recover human plasma, human blood was centrifuged at 2000 rpm for 15 min to separate the erythrocytes from the plasma. Human plasma was withdrawn and diluted at 1% v/v in 20 mM phosphate buffer pH 7,4 and NPs were added (1% w/v). The interaction with SANPs or SANPs-miRNA with serum proteins as well as the NPs aggregation were evaluated by monitoring the mean size of the both SANPs and SANP-miRNA formulations in BSA and human plasma up to 4 h at 37 °C. Each analysis was prepared in duplicate.

Hemolysis assay on SANPs and SANPs-miRNA has been performed on fresh human blood as previously reported by Mahmoud et al. (2014), with slight modifications. Briefly, the erythrocytes were collected from the plasma by centrifugation at 2000 rpm for 15 min, and then reconstituted in aqueous solution of NaCl 0,9% w/v. This step was repeated three times. The erythrocytes were diluted 1:10 with the solution of NaCl 0.9% (w/v) and then 0.2% (w/v) of formulations were added, mixed at 600 rpm for 30 s by vortex and incubated in a shaker bath at 37 °C for 4 h. The negative control (0% hemolysis) was obtained by diluting 1:10 human blood in NaCl 0.9% (w/v), whereas the positive control (100% hemolysis) was prepared by adding an excess of water to human erythrocytes, to induce lysis. Afterwards, the samples were withdrawn, placed on ice for 2 min to quench erythrocyte lysis and centrifuged (3000 rpm for 5 min) to separate the supernatant from the pellet, consisting of intact red blood cells. The obtained supernatant was centrifuged another time (3000 rpm for 5 min) and the content of hemoglobin was determined by spectrophotometer Thermo Fisher Scientific 1510 Multiskan Go measuring the absorbance (ABS) at $\lambda = 540$ nm. The percentage of hemolysis was calculated using the formula:

$$\text{Hemolysis \%} = ((\text{ABS}_{sample} - \text{ABS}_0)/(\text{ABS}_{100} - \text{ABS}_0))*100$$

where ABS_0 was the absorbance of the negative control and ABS_{100} the absorbance of the positive one.

2.2.5. Real-time quantitative PCR

Human GBM cell Lines LN229, U87MG were purchased by the American Type Culture Collection (ATCC). U87MG cells were cultured at 37 °C in a 5% CO_2 atmosphere in RPMI 1640 medium containing L-glutamine (Gibco®, Life Technologies, Carlsbad, CA) with the addition of 10% fetal bovine serum (FBS) decomplemented in the bath at 56 °C for 20 min (Lonza Group Ltd, Switzerland), 1% of a solution of penicillin and streptomycin (Gibco®, Life Technologies). LN229 cells were grown at 37 °C in a 5% CO_2 atmosphere, in a DMEM medium (Gibco®, Life Technologies, Carlsbad, CA), with the addition of 10% fetal bovine serum (FBS) added to bath at 56 °C for 20 min (Lonza Group Ltd, Switzerland), 1% of L-glutamine, 1% of penicillin and streptomycin (Gibco®, Life Technologies). Cell transfection efficiency was evaluated by Real-time quantitative PCR using ViiA 7 System (Applied Biosystems, California, USA). Cells were transfected or not with miR603 or treated with different formulations of nanoparticles containing miR603 at a concentration of 50 nM. After 24, 48, 72 h, total RNA from suspension cell line LN229 and U87MG (5×10^5 cells) was obtained by mirVana miRNA Isolation Kits (Ambion, Life Technologies, California, USA) according to manufacturer's instructions. The integrity, quality and quantity of RNA were assessed by the NanoDrop ND-1000 Spectrophotometer (Thermo Fisher Scientific, Wilmington, DE, USA). Oligo-dT-primed cDNA was obtained using the High Capacity cDNA Reverse Transcription Kit (Applied Biosystems). The single-tube TaqMan miRNA assays (Ambion, Life Technologies, California, USA) was used to detect and quantify mature miR603 according to the manufacturer's instructions by the real-time PCR ViiA7 (Applied Biosystems, California, USA). MiR603 expression was normalized on U-6 (Ambion, Life Technologies, California, USA). Comparative real-time PCR (RT-PCR) was performed in triplicate, including no template
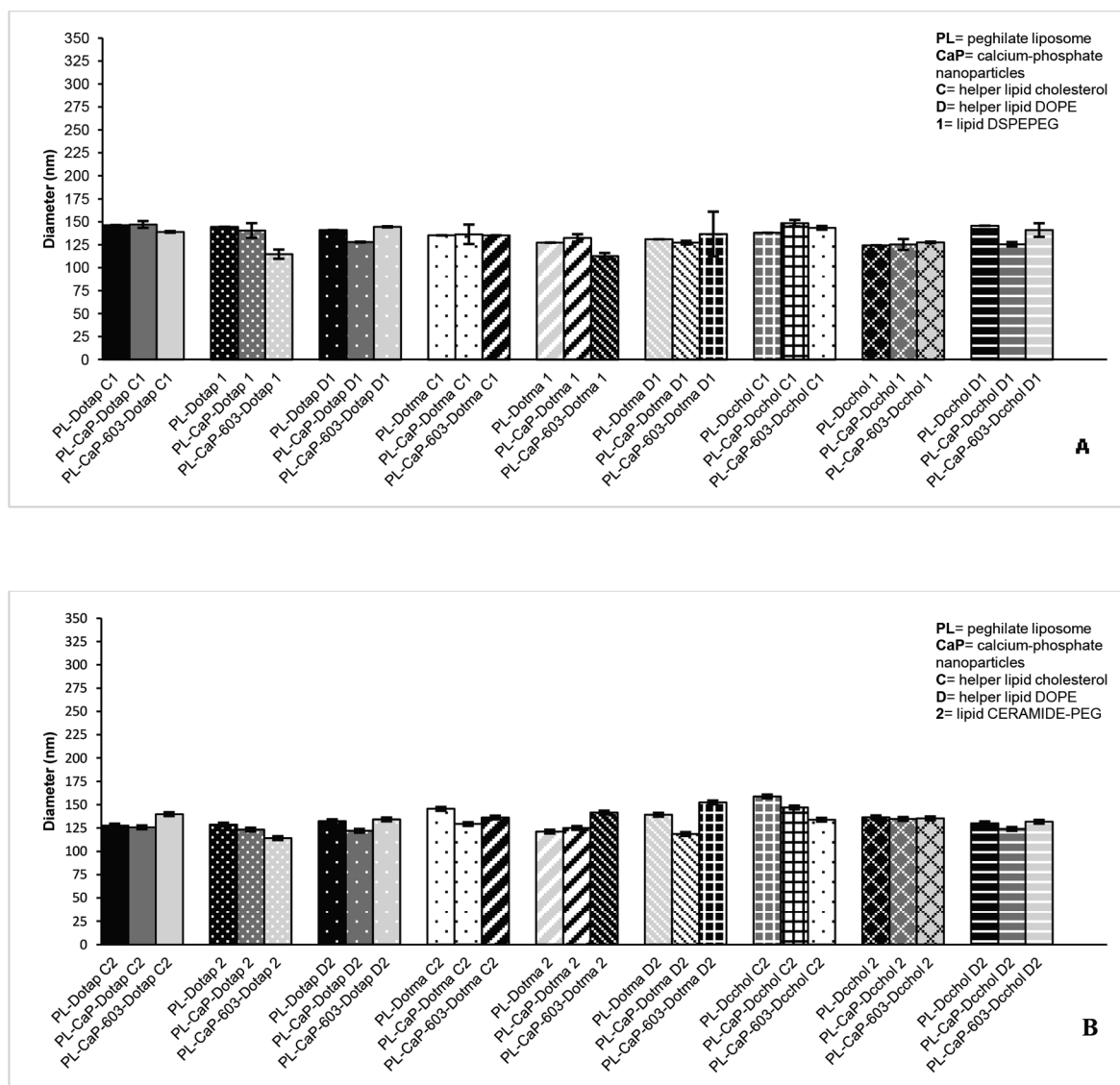
Fig. 2. Mean diameter (nm) of the PEGylated liposomes and SANPs before and following complexation with miR603. PL = PEGylated liposomes; SANPs = hybrid self-assembling nanoparticles. C = cholesterol; D = DOPE; 1 = DSPE-PEG$_{2000}$; 2 = cer-PEG$_{2000}$. Panel A: formulations containing DSPE-PEG$_{2000}$; Panel B: formulations containing cer-PEG$_{2000}$.

controls, and relative expression was calculated using the comparative cross-threshold (Ct) method.

2.2.6. Cell viability assay

We assessed the viability of the cell lines using a colorimetric assay that measures the ability of viable cells to transform a soluble tetrazolium salt (MTT) to an insoluble purple formazan precipitate. Cells were plated at the appropriate density in 96-well microtitre plates. After 24 h, cells were exposed to various concentrations of different formulations of nanoparticles to test their cytotoxicity. After 72 h, 10 µL of MTT (1 mg·mL-1) and 200 µL of medium were added to the cells in each well. After 4 h incubation at 37 °C, the medium was removed, then the formazan crystals were solubilized by adding 100 µL of DMSO and by mixing it in an orbital shaker for 20 min. Absorbance at 570 nm was measured using a plate reader. Experiments were performed in triplicate. As a control, 0.5% DMSO was added to untreated cells. Data were expressed as mean ± SD.

2.2.7. In vivo experiments

SCID male mice (5–6 weeks old) purchased from Charles River (Calco, Italy) were injected intracranially with U87MG human GBM line at 2.5 × 10^5 cells/mouse and after two weeks mice were treated

intravenously with 6.8 µg miR603/mouse of two different SANPs-miRNA that are, PL-CaP-603-DOTAP-C1, composed of CaP and PLs consisting of DOTAP/CHOL/DSPE-PEG mM ratio 1:1.8:0.125), and PL-CaP-603-DOTAP-2, composed CaP and PLs of DOTAP/cer-PEG (mM ratio 1:0.125) formulations. Mice were euthanized 6 h and 18 h after the treatment and plasma and organs collected and maintained at −80 °C until analysis. All animal experiments comply with the ARRIVE guidelines and have been be carried out in accordance with EU Directive 2010/63/EU for animal experiments.

2.2.8. RNA extraction on mouse biopsies and Real-time quantitative PCR

Total RNA was extracted from mouse biopsies by mirVana miRNA Isolation Kits (Ambion, Life Technologies, California, USA) according to manufacturer's instructions as follows. In details, tissues were homogenized in 300 µL of Disruption Buffer. Successively, an equal volume of Denaturing Buffer (previously set at 37 °C) was added to the tissues homogenate and they were incubated in ice for 5–10 min. Then, Phenol-chloroform was added in the tube in a volume equal to the total volume and centrifugated at 10,000 rcf for 5 min. After centrifugation, the aqueous phase was collected and a volume of absolute ethanol equal to 1.25 times that of the collected volume was added. Then
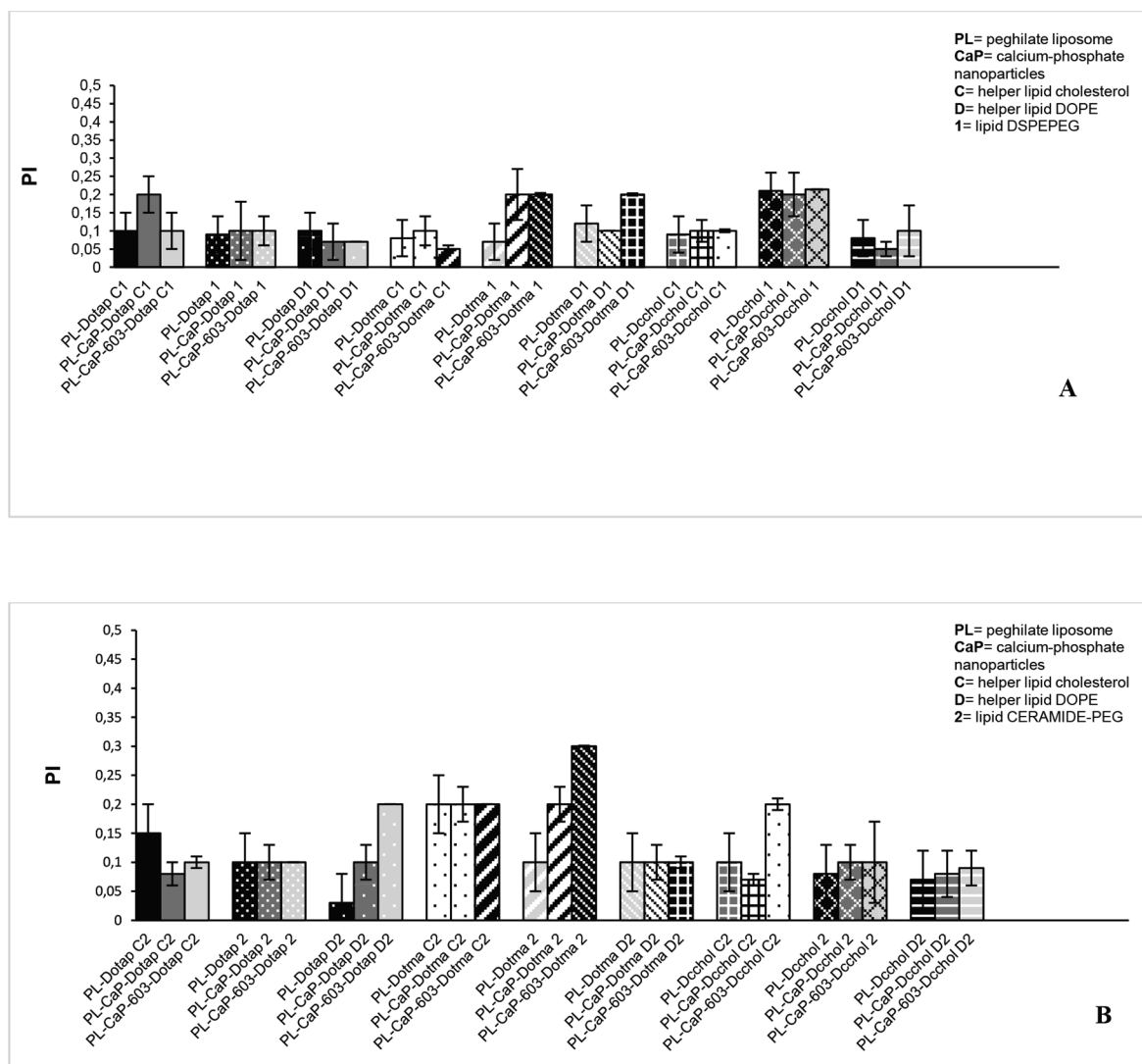
Fig. 3. Polydispersity index (PI) of the PEGylated liposomes and SANPs before and following complexation with miR603. PL = PEGylated liposomes; SANPs = hybrid self-assembling nanoparticles. C = cholesterol; D = DOPE; 1 = DSPE-PEG$_{2000}$; 2 = cer-PEG. Panel A: formulations containing DSPE-PEG$_{2000}$; Panel B: formulations containing cer-PEG$_{2000}$.

700 μL at a time were collected, applied in Filter Cartridge and centrifuged at 10,000 rcf for 5 min. 700 μL of Wash Solution 1 were added on each Filter Cartridge, followed by centrifugation at 10,000 rcf for 40 s, later two washings with 500 μL of Wash Solution 2 were performed. Finally, 50 μL of Eluition Buffer (preheated at 95 °C) were added to the Filter Cartridge, previously placed on new tubes. Then, the samples were quantized to Nanodrop (Technologies Inc., Wilmington, DE). cDNA was obtained by using the TaqMan® Small RNA Assays Kit (Applied Biosystems) according to the manufacturer's instructions. The single-tube TaqMan miRNA assays (Ambion, Life Technologies, California, USA) was used to detect and quantify mature miR603 according to the manufacturer's instructions by the use of the Real-time PCR ViiA7 (Applied Biosystems, California, USA). MiR603 expression was normalized on U-6 (Ambion, Life Technologies, California, USA). Comparative real-time PCR (RT-PCR) was performed in triplicate, including no template controls, and relative expression was calculated using the comparative cross-threshold (Ct) method.

3. Results and discussion

SANPs are core–shell nanoparticles obtained by a self-assembling process and designed for an easy scale-up and to facilitate the technology transfer (Campani et al., 2018). However, while for bisphosphonates the usefulness of this technology has been largely showed (Salzano et al., 2011; Marra et al., 2012; Salzano et al., 2016), the possibility to use SANPs for the delivery of other chemical species, e.g. nucleic acids, remains to be demonstrated. Thus, in this study, the potential of SANPs for the delivery of nucleic acids was investigated. In particular, a specific miRNA, e.g. miR603, was used as model miRNA, but also for its potential to revert chemoresistance in the treatment of GBM (Kushwaha et al., 2014). Due to the potentialities of miR603, the ability of SANPs to deliver the miRNA in GBM, *in vitro* and *in vivo*, was studied. SANPs encapsulating miRNA with optimized characteristics in term of size, zeta potential, physical stability in biological media, low hemolytic activity, were developed. To this aim, lipid composition, namely the type of cationic lipid, the presence of a neutral lipid and the type of PEGylated lipid were optimized.

Three different cationic lipids largely used for transfection purposes, namely DOTAP, DOTMA and DC-chol, were tested in this study. Cationic lipids were used to "anchor" the lipid shell to the inorganic core of the SANPs, but also as transfection agent for the nucleic acid. Each cationic lipid was used alone or associated to two different neutral lipids, namely CHOL and DOPE. CHOL has been used to improve the transfection efficiency of cationic liposomes (De Rosa et al., 2008;
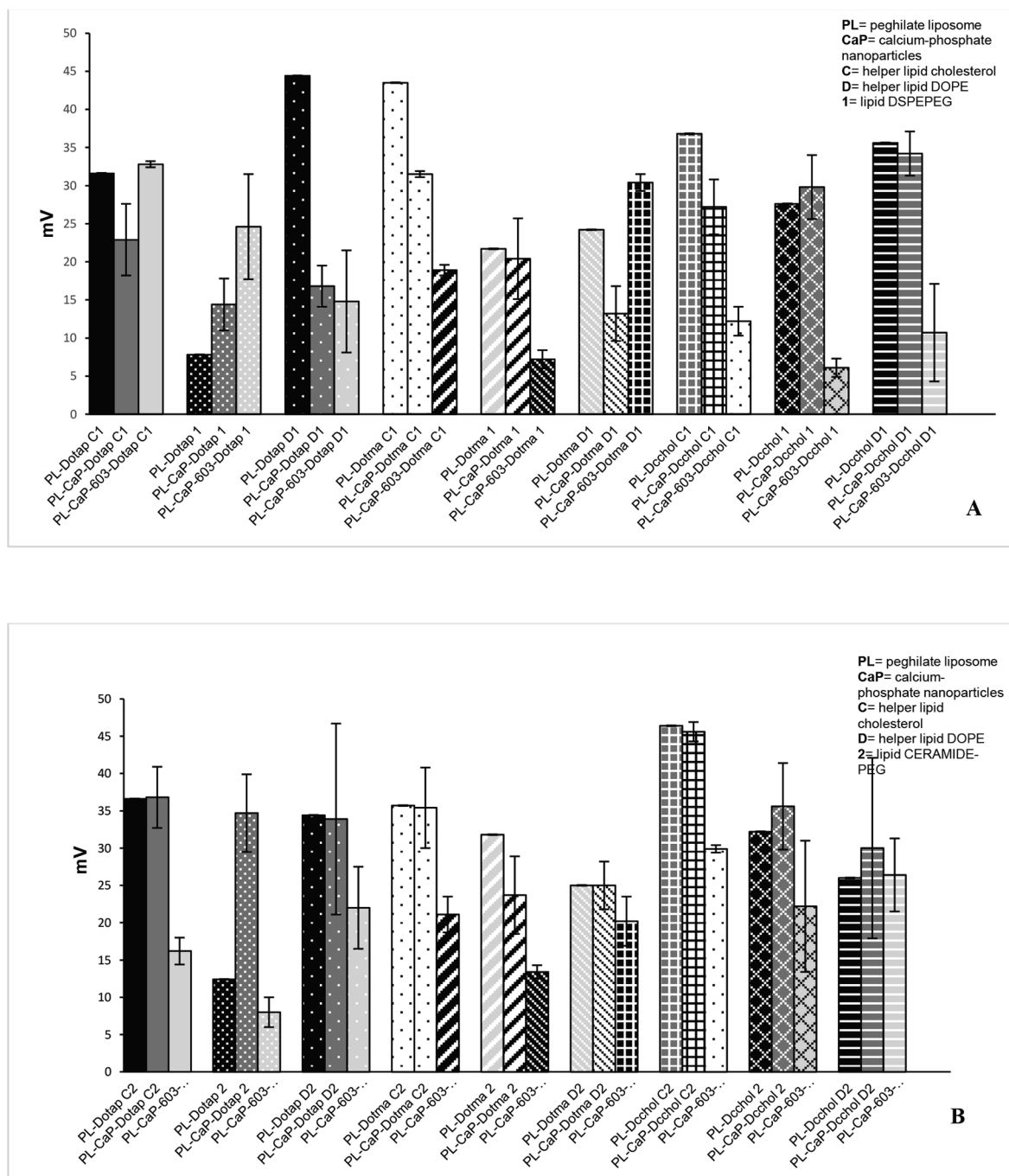
Fig. 4. Zeta potential (ζ) of the PEGylated liposomes and SANPs before and following complexation with miR603 and miR603 O-Met. PL = PEGylated liposomes; SANPs = hybrid self-assembling nanoparticles. C = cholesterol; D = DOPE; 1 = DSPE-PEG$_{2000}$; 2 = cer-PEG. Panel A: formulations containing DSPE-PEG$_{2000}$; Panel B: formulations containing cer-PEG$_{2000}$.

Hosseini et al., 2019). Similarly, the addition of the fusogenic lipid DOPE to the formulation is considered a well-established strategy to promote the escape of nucleic acids from endosomes (Litzinger and Huang, 1992; Khatri et al., 2014). Moreover, it has been demonstrated that the introduction of "helper lipids", such as DOPE or CHOL, can stabilize the carrier membrane, reducing vesicle aggregation in the presence of serum proteins (Xiong et al., 2011). Finally, in all the formulations, a PEGylated lipid, namely DSPE-PEG$_{2000}$ or cer-PEG$_{2000}$, was included. The inclusion of a PEGylated shell on the liposome surface has been used to increase the stability of SANPs-miRNA in biological fluids (Jiang et al., 2010). The higher stability in serum results in an increased circulation time of the formulations (Maeda et al., 2000)

also due to a reduction of uptake by macrophages. Thus, PEGylation of SANPs-miRNA could encourage the transfection efficiencies in relevant biological media (Balazs and Godbey, 2011; Xue et al., 2015).

In Table 1, the composition of all the SANP formulations prepared in this study is summarized.

3.1. Physical-chemical characterization of SANPs

Mean diameter, polydispersity index and surface charge of PLs, plain SANPs and SANPs-miRNA (also called PL-CaP and PL-CaP-603 respectively into the charts and tables) are reported in Figs. 2–4, respectively.

Table 2

Encapsulation of miRNA into the different SANP formulations (expressed as amount of mmol of miRNAs/mmol of cationic lipid), encapsulation efficiency (expressed as percentage respect to the miRNA initially used in the formulations); hemolytic activity and cytotoxicity of the different SANPs on LN229 and U87MG (for more information see the section Materials and Methods). C = cholesterol; D = DOPE; 1 = DSPE-PEG$_{2000}$; 2 = cer-PEG$_{2000}$.

Formulation	miRNA encapsulation		Hemolysis %	Cytotoxicity – IC50 (nM)	
	mmol miRNA/mmol cationic lipid	miRNA encapsulation efficiency (%)		U87MG	LN229
PL-CaP-603-DOTAP C1	1.52 ± 0.00	100 ± 0.0	1.11 ± 0.003	No toxic	No toxic
PL-CaP-603-DOTAP 1	1.42 ± 0.00	100 ± 0.0	0.08 ± 0.004	No toxic	No toxic
PL-CaP-603-DOTAP D1	1.53 ± 0.00	100 ± 0.0	0.19 ± 0.005	No toxic	No toxic
PL-CaP-603-Dotma C1	1.53 ± 0.00	100 ± 0.0	2.45 ± 0.006	176.9	171.0
PL-CaP-603-Dotma 1	1.53 ± 0.00	100 ± 0.0	1.46 ± 0.002	No toxic	No toxic
PL-CaP-603-Dotma D1	1.53 ± 0.00	100 ± 0.0	1.12 ± 0.004	Highly toxic	Highly toxic
PL-CaP-603-Dcchol C1	1.53 ± 0.00	99 ± 0.2	0.73 ± 0.011	Highly toxic	Highly toxic
PL-CaP-603-Dcchol 1	1.24 ± 0.00	81 ± 0.0	0.21 ± 0.001	Highly toxic	Highly toxic
PL-CaP-603-Dcchol D1	1.52 ± 0.00	99 ± 0.4	0.07 ± 0.002	Highly toxic	Highly toxic
PL-CaP-603-DOTAP C2	1.53 ± 0.00	100 ± 0.4	0.09 ± 0.003	No toxic	No toxic
PL-CaP-603-DOTAP 2	1.26 ± 0.10	82 ± 6.4	1.00 ± 0.013	No toxic	No toxic
PL-CaP-603-DOTAP D2	1.16 ± 0.31	75 ± 19.8	1.72 ± 0.008	No toxic	85.6
PL-CaP-603-DOTMA C2	1.53 ± 0.00	100 ± 0.0	6.13 ± 0.019	142.1	159.3
PL-CaP-603-DOTMA 2	1.53 ± 0.00	100 ± 0.0	16.74 ± 0.033	156.0	182.5
PL-CaP-603-DOTMA D2	1.53 ± 0.00	100 ± 0.0	5.23 ± 0.060	Highly toxic	Highly toxic
PL-CaP-603-DCchol C2	1.31 ± 0.00	100 ± 0.0	2.38 ± 0.030	Highly toxic	Highly toxic
PL-CaP-603-DCchol 2	1.47 ± 0.00	96 ± 0.0	1.98 ± 0.014	Highly toxic	Highly toxic
PL-CaP-603-DCchol D2	1.48 ± 0.01	96 ± 0.6	1.97 ± 0.012	Highly toxic	Highly toxic

PLs had a mean diameter ranging between about 120 and 160 nm. The complexation of PLs with the CaP dispersion resulted in plain SANPs with a mean diameter generally around 140 nm and a PI between about 0.05 and 0.2, suggesting that the lipid composition has no a significant effect on the SANPs size. On the case of liposomes based on the cationic lipid and PEGylated lipid, the size and the consequent high curvature of the bilayer could lead to the localization of PEGylated lipids on the outer layer of the membrane, thus shielding the positive charge of the cationic lipid. On the other hand, the inclusion of neutral lipids could contribute to the reorganization of the bilayer shifting toward a more homogeneous distribution of PEGylated lipid between the outer and the inner layers of the membrane, and consequent increase of the ζ value.

The addition of the miRNA to plain SANPs did not significantly affect the mean size, with a weak effect on the PI that remains under 0.2, with the exception of the formulation containing DOTMA and cer-PEG$_{2000}$ (PI ~ 0.3), (Fig. 3).

Moreover, the encapsulation of miRNA influenced the ζ, being this effect strictly depending on the formulation (Fig. 4). In particular, in the majority of the formulations, a reduced ζ was found, suggesting that the anionic charged miRNA interact with the cationic lipid, also at the level of the external lipid shell. In the formulations PL-CaP-603-Dotap1 and PL-CaP-603 DotmaD1, the inclusion of miRNA lead to increase of zeta potential; this could be ascribed to the lipid rearrangement inducing the shielding of the cationic charges by the PEGylated lipids.

In Table 2, the amount of miRNA encapsulated, expressed as miRNA actual loading (mmol of miRNAs/mmol of cationic lipid) and miRNA encapsulation efficiency (expressed as percentage respect to the miRNA initially used in the formulations) in the SANPs-miRNA is reported. All the formulations were characterized by a very high miRNA encapsulation efficiency, ranging from about 72 to 100%, the lowest encapsulation being observed in the case of the formulation based on DOTAP, DOPE and cer-PEG$_{2000}$. The comprehension of the lipid rearrangement and SANPs architecture affecting the efficiency of the miRNA complexation are very complex and cannot clarified in this study. However, we can hypothesize that SANPs with the lowest encapsulation efficiency are characterized by a more compact structure that limits the complexation and encapsulation of large amount of miRNA

In a second phase of the study, considering that the SANPs-miRNA are designed for an intravenous administration, the SANPs physical stability was tested firstly in a BSA solution at 1% w/v (for a first screening) and then in human plasma up to 4 h at 37 °C. The aggregation of SANPs-miRNA in presence of serum proteins was evaluated by monitoring the mean size of the formulations (1% w/v) in both media. SANPs mean diameter in both media is reported in the Fig. 5.

All the formulations did not significantly change their mean size following incubation in BSA for 4 h. On the contrary, the stability of SANPs-miR603 in human plasma strictly depended on the formulation. Significant increase in size, presumably aggregation, was found in formulations combining DOTMA and cer-PEG$_{2000}$. Moreover, the formulations with DC-chol associated to cholesterol and cer-PEG$_{2000}$ was found to aggregate in plasma. It is well known that ceramide can interact with the hydrophobic portion of proteins (Krönke, 1999). The higher propensy of some SANPs containing cer-PEG$_{2000}$ to interact with proteins (probably different than BSA) can lead to particle aggregation.

3.2. Hemolytic activity of SANPs-miRNA

The hemolytic activity of SANPs-miRNA was then evaluated in human blood. In particular, according to ASTM F 756-17, a hemolytic activity less than 2% was considered non-toxic, while at levels between 2 and 5% only slightly toxic. As reported in Table 2, SANPs-miRNA showed a different hemolytic effect depending on the composition. In particular, the combination of DOTMA and cer-PEG$_{2000}$ led always to a hemolytic activity from slight to important (from 3% to 16%). For all the other formulations, hemolytic values close or lower than 2% were observed, suggesting no toxicity on the red blood cells. Previous studies underlined the relationship between physical stability of nanoparticles and their hemocompatibility (Vuddanda et al., 2014; Jansook et al., 2018). In this study, also formulations, e.g. SANPs-miR603-DOTMA 2 and SANPs-miR603-DOTMA D2, that were stable in presence of proteins, showed significant hemolytic activity. Thus, in this case, a direct interaction of the SANPs with the membrane of red blood cells should be hypothesized. Once more, this interaction could be enhanced by the presence of cer-PEG$_{2000}$ that can enhance membrane propensity to form a hexagonal II phase, thus changing the membrane fluidity, which may impinge on fusion processes with cell membrane (Krönke, 1999), e.g. membrane of red blood cells.

3.3. Cytotoxicity of SANPs

The cytotoxicity of the SANP formulations at different concentrations, namely from 20 to 200 nM, was tested on two glioblastoma cell
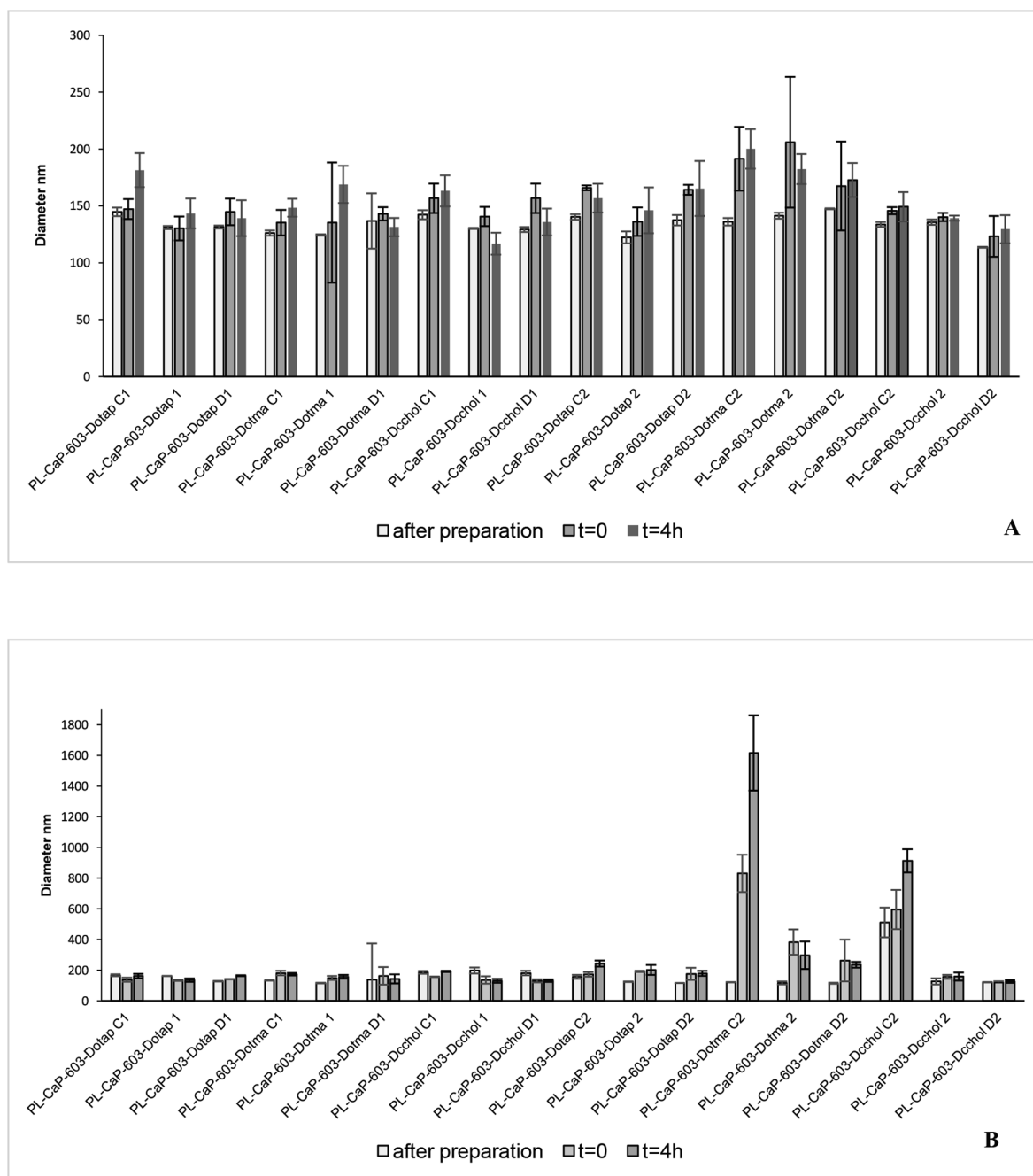
Fig. 5. Stability of SANPs-miR603 in bovine serum albumin (BSA), (panel A) and in human plasma, (panel B), after incubation (t = 0) and after four hours (t = 4). C = cholesterol; D = DOPE; 1 = DSPE-PEG$_{2000}$; 2 = cer-PEG.

lines, e.g. LN229 and U87MG. The formulations showing a cell viability lower than 80% at 100 nM were considered "highly toxic". Formulations showing a cell viability lower than 80% of at the 200 nM, but higher than 80% at 100 nM, were considered "slightly toxic". Formulations showing on both cell lines 80% of cell viability at the highest concentration (200 nM) were considered not toxic in our experimental conditions. The non-toxic SANPs were used for the following phase of the study. The results are summarized in Table 2. When considering the different cationic lipid used in this study, DOTMA and DC-chol based formulations were generally found from slightly to very toxic. Other authors found a higher cytotoxicity in vitro when using lipoplexes based on DC-chol (Lechanteur et al., 2018), compared to DOTAP. Similarly, the higher cytotoxicity of DOTMA compared to the DOTAP has previously been reported and reasonably attributed to the

biodegradable ester bond present only in the latter (Obika et al., 1999). DOTAP-based SANPs were found not toxic on both the cell lines, when prepared with DSPE-PEG. The use of cer-PEG, only in the formulation containing DOPE, led to a slight toxicity (IC50 of 86 nM) found on LN229 cells.

Taking into account these data, we considered that the formulations based on DOTAP, alone or associated with chol, were stable in serum, have no hemolytic activity, and were not cytotoxic; these formulations were used in the following step of the study.

3.4. Delivery of miR603 in GBM cell lines

The selected formulations were used to deliver miR603 in LN229 and U87MG. The uptake of miR603 was measured by RT-PCR after 24
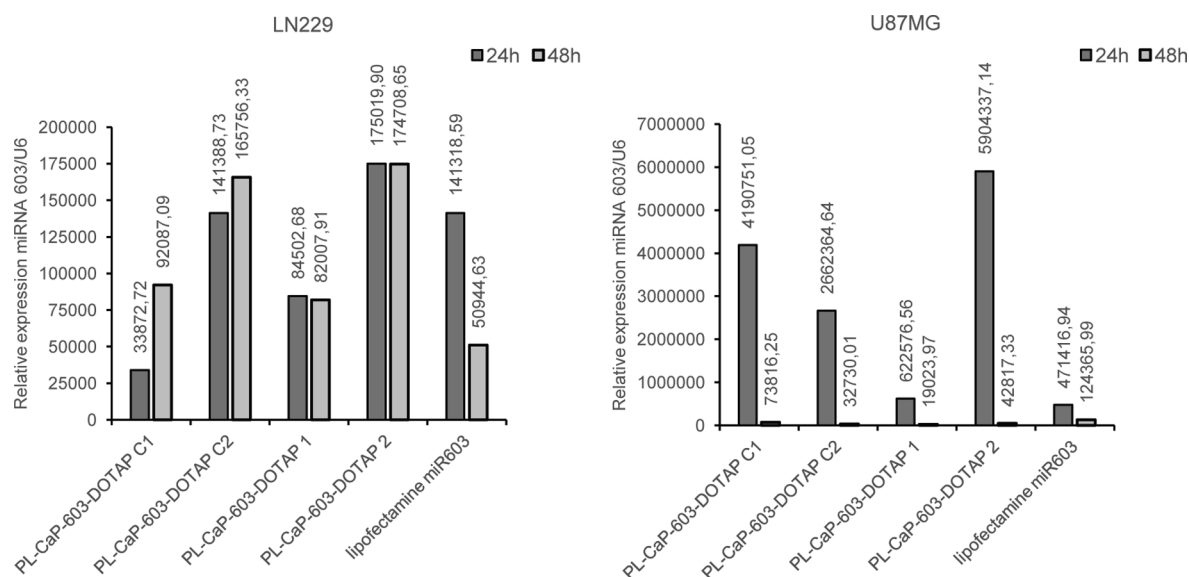
Fig. 6. Intracellular uptake of miR603, measured by RT-PCR, after 24 and 48 h of LN229 (left panel) and U87MG (right panel) incubation with the formulations. Lipofectamine was used for comparison purpose.
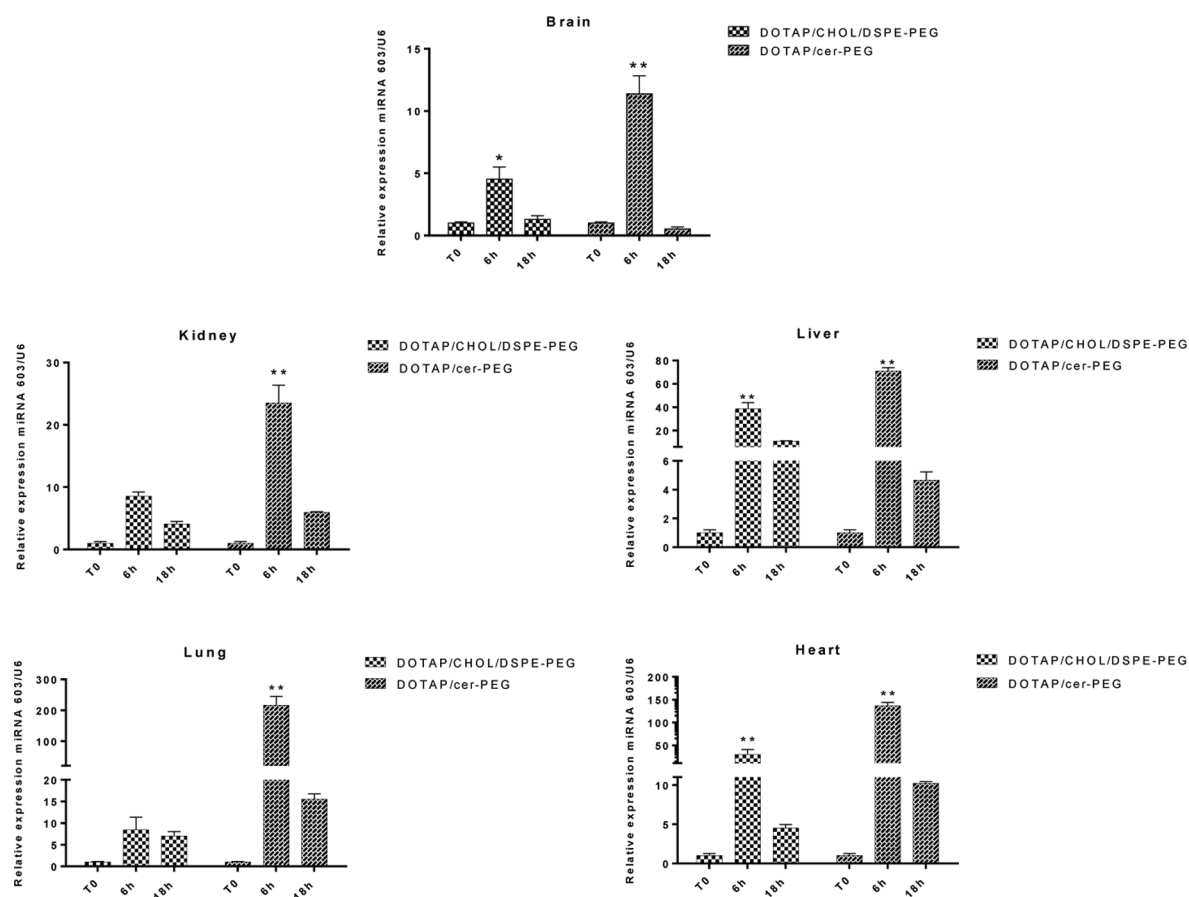

Fig. 7. Levels of miR603 accumulated in brain, lungs, kidneys, heart, and liver before or following 6 and 18 h from the administration of PL-CaP-603-DOTAP C1 and PL-CaP-603-DOTAP 2 formulations.

and 48 h of cell incubation with the formulations. As positive control, the commercial transfection agent lipofectamine was used. Transfection with lipofectamine lead to a significant miR603 uptake in both LN229 and U87MG (Fig. 6). In the case of w.t. miR603 delivered with lipofectamine, the highest miRNA uptake was found after incubation for 24 h, while miR603 levels progressively reduced after 48 and 72 h of

incubation, respectively. This suggests a very poor miR603 stability into the cells following transfection, although this point should be further investigated. The cell incubation with SANPs encapsulating the miR603 led to a strong increase of the miR603 uptake into the cells (Fig. 6). In particular, in LN229 cells the formulation SANPs-603-DOTAP 2 lead to a significant improvement of the miR603 uptake after 24 and 48 h of

incubation. Interestingly, a higher level of miRNA was found following 48 h of incubation with SANPs-603-DOTAP C1 and DOTAP/DSPE-PEG, suggesting that the release of naked miR603 into the cells could be delayed with this formulation (Fig. 6, left panel). In the case of U87MG (Fig. 6, right panel), the miR603 uptake into the cells increased from 1.2 to 12.5 times depending on the SANP formulations used. As in the case of LN229, the highest miRNA delivery was observed with the formulation DOTAP/cer-PEG. However, in the case of U87MG, the intracellular level of miR603 was found very low following 48 h of incubation. Thus, it could be hypothesized that a "sustained release" of miRNA into LN229 occurs, while in the case of U87MG a faster and higher delivery takes place, with consequent faster intracellular degradation of the miR603 into the cells.

The higher delivery of miRNA found in the case of SANPs based on DOTAP/cer-PEG could be ascribed to the role of cer-PEG. Previously, other authors compared the use of cer-PEG$_{2000}$ and DSPE-PEG in lipoplexes encapsulating siRNA, demonstrating superior transfection in the case former (Lechanteur et al., 2016). In the case of lipoplexes, it has been reported that cationic lipids and RNA can adopt a lamellar or a hexagonal phase (Smisterová et al., 2001), being the latter the most favourable to the transfection and in particular to the endosomal escape of RNA (Rädler et al., 1997; Koltover et al., 1998; Dan and Danino, 2014). Shi et co-workers demonstrated that DSPE-PEG stabilize the lipoplexes in lamellar phase whereas cer-PEG$_{2000}$ favour the hexagonal organization (Shi et al., 2002). Finally, it has been suggested that cer-PEG$_{2000}$ provide a steric hindrance of PEG chain lower than DSPE-PEG, thus promoting endosomal escape of siRNA (Lechanteur et al., 2016). It is worthy of note that lipofectamine, used in this study for comparison purpose, consists on non-PEGylated liposomes that should provide higher transfection compared to PEGylated lipid nanoparticles. SANPs used in this study are PEGylated lipid nanoparticles and provided a transfection efficiency up to about 400 times higher than lipofectamine. To explain the high delivery efficiency of SANPs, we could hypothesize that also the CaP components could play a role. The potential of calcium phosphate nanoparticles as transfection agents has been largely reported (Mostaghaci et al., 2016; Xu et al., 2016). Colloidal calcium phosphate particles have also endosomal escape properties that could be beneficial in the miRNA delivery by SANPs (Ma, 2014) in combination with the cationic lipid.

3.5. Biodistribution of miR603 encapsulated in SANPs

The ability of the selected SANP formulations to deliver *in vivo* miR603 was also investigated. In particular, the biodistribution of miRNA encapsulated in SANPs with different lipid compositions, namely SANPs-603-DOTAP C1 composed of DOTAP/CHOL/DSPE-PEG (mM ratio 1:1.8:0.125) and SANPs-603-DOTAP 2 composed of DOTAP/cer-PEG (mM ratio 1:0.125), has been studied in an orthotopic model of GBM. RNA distribution in brain, lungs, kidneys, heart, and liver has been studied before (time zero) and following 6 and 18 h from the SANPs administration. The results are reported in Fig. 7. Independently on the formulation, the highest levels of miR603 were found at 6 h from the administration. Different levels of miR603 were observed in the different organs with the highest levels found in the lungs. Interestingly, miR603 levels were significantly affected by the formulation, with the highest accumulation always in the case of the formulation SANP-603-DOTAP 2. In particular, when compared with the formulation DOTAP/CHOL/DSPE-PEG, the use of the formulation based on DOTAP/cer-PEG allowed to achieve more than two times higher miR603 accumulation into the brain. This difference was also larger in the case of the other organs, especially in the case of lung where one order of magnitude of miR603 accumulation was found. These data are in agreement with previous works carried out in an orthotopic model of GBM where SANP accumulation into the cerebral tumor was found at 6 h following the first administration (Porru et al., 2014). Thus, it is reasonable to hypothesize that also SANP encapsulating miRNA not

only reach the brain, but also accumulate into the tumor.

All together these results suggest that SANPs technology can be successfully proposed as delivery system for non-coding RNA (e.g. siRNA or miRNA). In particular this study provides insights for the optimization of lipid composition combining small size, high RNA encapsulation, stability in presence of plasma protein, hemocompatibility, low cytotoxicity, high transfection efficiency and *in vivo* delivery in different organs, including into the brain in a relevant orthotopic model of GBM.

4. Conclusions

This study provides the proof-of-principle to further boost the study of the SANPs as promising delivery tool for nucleic acids, e.g. miRNA. The finding underlines that the use of the cationic lipid into SANPs is not only mandatory for anchoring the lipid shell to the core, but also able to influence SANPs architecture, physical and biological stability, and the delivery process. Among the neutral lipid used here, the DOPE provided a slight toxicity in some formulations, thus only SANPs based on DOTAP and DOTAP/chol were selected. Finally, the use of cer-PEG$_{2000}$ provided the highest delivery efficiency, compared to the DSPE-PEG. Biodistribution study underlined that such SANPs are able to deliver miRNA in different organs but allowing also accumulation of significant levels of the nucleic acid in the brain in an orthotopic model of GBM. Further studies will clarify if the amounts of miRNA delivered in the different organs, e.g. into the brain, will allow to achieve a pharmacological effect.

CRediT authorship contribution statement

Virginia Campani: . : Conceptualization, Methodology, Investigation, Data curation, Writing - review & editing. **Silvia Zappavigna:** Formal analysis, Investigation, Data curation. **Lorena Scotti:** Validation, Formal analysis, Data curation, Writing - original draft, Visualization. **Marianna Abate:** Methodology, Investigation. **Manuela Porru:** Data curation, Investigation, Formal analysis, Writing - original draft. **Carlo Leonetti:** Resources, Supervision. **Michele Caraglia:** Resources, Supervision. **Giuseppe De Rosa:** Conceptualization, Resources, Supervision, Project administration, Funding acquisition.

Declaration of Competing Interest

The authors declare that they have no known competing financial interests or personal relationships that could have appeared to influence the work reported in this paper.

Acknowledgements

References

Balazs, D.A., Godbey, W., 2011. Liposomes for use in gene delivery. J. Drug Deliv. 32649, 7. https://doi.org/10.1155/2011/326497.

Campani, V., De Rosa, G., Misso, G., Zarone, M.R., Grimaldi, A., 2016. Lipid nanoparticles to deliver miRNA in cancer. Curr. Pharm. Biotechnol. 17 (8), 741–749. https://doi.org/10.2174/1389201017086517234941.

Campani, V., Giarra, S., De Rosa, G., 2018. Lipid-based core-shell nanoparticles: evolution and potentialities in drug delivery. OpenNano 3, 5–17.

Dan, N., Danino, D., 2014. Structure and kinetics of lipid-nucleic acid complexes. Adv. Colloid Interface Sci. 205, 230–239. https://doi.org/10.1016/j.cis.2014.01.013.

De Rosa, G., De Stefano, D., Laguardia, V., Arpicco, S., Simeon, V., Carnuccio, R., Fattal, E., 2008. Novel cationic liposome formulation for the delivery of an oligonucleotide

decoy to NF-kappaB into activated macrophages. Eur. J. Pharm. Biopharm. 70 (1), 7–18. https://doi.org/10.1016/j.ejpb.2008.03.012.

Etheridge, M.L., Campbell, S.A., Erdman, A.G., Haynes, C.L., Wolf, S.M., McCullough, J., 2013 Jan. The big picture on nanomedicine: the state of investigational and approved nanomedicine products. Nanomedicine 9 (1), 1–14. https://doi.org/10.1016/j.nano.2012.05.013.

Hosseini E.S., Nikkhah M., Hosseinkhani S., Cholesterol-rich lipid-mediated nanoparticles boost of transfection efficiency, utilized for gene editing by CRISPR-Cas9, Int. J. Nanomed., 2019; 14:4353-4366. doi: 10.2147/IJN.S199104.

Jansook, P., Pichayakorn, W., Ritthidej, G.C., 2018. Amphotericin B-loaded solid lipid nanoparticles (SLNs) and nanostructured lipid carrier (NLCs): effect of drug loading and biopharmaceutical characterizations. Drug Dev. Ind. Pharm. 44 (10), 1693–1700. https://doi.org/10.1080/03639045.2018.1492606.

Jiang, J., Yang, S.J., Wang, J.C., Yang, L.J., Xu, Z.Z., Yang, T., Liu, X.Y., Zhang, Q., 2010. Sequential treatment of drug-resistant tumors with RGD-modified liposomes0 containing siRNA or doxorubicin. Eur. J. Pharm. Biopharm. 76 (2), 170–178. https://doi.org/10.1016/j.ejpb.2010.06.011.

Kanasty, R., Dorkin, J.R., Vegas, A., Anderson, D., 2013 Nov. Delivery materials for siRNA therapeutics. Nat. Mater. 12 (11), 967–977. https://doi.org/10.1038/nmat3765.

Khatri, N., Baradia, D., Vhora, I., Rathi, M., Misra, A., 2014. Development and characterization of siRNA lipoplexes: Effect of different lipids, in vitro evaluation in cancerous cell lines and in vivo toxicity study. AAPS PharmSciTech 15, 1630–1643. https://doi.org/10.1208/s12249-014-0193-9.

Koltover, I., Salditt, T., Rädler, J.O., Safinya, C.R., 1998. An inverted hexagonal phase of cationic liposome-DNA complexes related to DNA release and delivery. 3;281(5373):78–81. Science. https://doi.org/10.1126/science.281.5373.78.

Krönke, M., 1999. Biophysics of ceramide signaling: interaction with proteins and phase transition of membranes. Chem. Phys. Lipids 101 (1), 109–121.

Kushwaha, D., Ramakrishnan, V., Ng, K., Steed, T., Nguyen, T., Futalan, D., Akers, J.C., Sarkaria, J., Jiang, T., Chowdhury, D., Carter, B.S., Chen, C.C., 2014. A genome-wide miRNA screen revealed miR-603 as a MGMT-regulating miRNA in glioblastomas. Oncotarget 5 (12), 4026–4039. https://doi.org/10.18632/oncotarget.1974.

Lechanteur, A., Furst, T., Evrard, B., Delvenne, P., Hubert, P., Piel, G., 2016. PEGylation of lipoplexes: the right balance between cytotoxicity and siRNA effectiveness. Eur. J. Pharma. Sci. 10 (93), 493–503. https://doi.org/10.1016/j.ejps.2016.08.058. E.

Lechanteur, A., Sanna, V., Duchemin, A., Evrard, B., Mottet, D., Piel, G., 2018. Cationic liposomes carrying siRNA: impact of lipid composition on physicochemical properties, cytotoxicity and endosomal escape. Nanomaterials 8 (5), 270. https://doi.org/10.3390/nano8050270.

Li, et al., 2010. Biodegradable calcium phosphate nanoparticle with lipid coating for systemic siRNA delivery. J. Control Release 142 (3), 416–421.

Litzinger, D.C., Huang, L., 1992. Biodistribution and immunotargetability of ganglioside-stabilized dioleoylphosphatidylethanolamine liposomes. Biochim. Biophys. Acta 1104 (1), 179–187. https://doi.org/10.1016/0005-2736(92)90148-f.

Ma, D., 2014. Enhancing endosomal escape for nanoparticle mediated siRNA delivery. Nanoscale 6 (12), 6415–6425. https://doi.org/10.1039/c4nr00018h.

Maeda, H., Wu, J., Sawa, T., Matsumura, Y., Hori, K., 2000. Tumor vascular permeability and the EPR effect in macromolecular therapeutics: a review. J. Control Release 65 (1–2), 271–284. https://doi.org/10.1016/s0168-3659(99)00248-5.

Mahmoud, D.B., Shukr, M.H., Bendas, E.R., 2014. In vitro and in vivo evaluation of self-nanoemulsifying drug delivery systems of cilostazol for oral and parenteral administration. Int. J. Pharm. 476 (1–2), 60–69. https://doi.org/10.1016/j.ijpharm.2014.09.045.

Marra M., Salzano G., Leonetti C., Porru M., Franco R., Zappavigna S ., Liguori G., Botti G., Chieffi P., Lamberti M., Vitale G., Abbruzzese A., La Rotonda M.I., De Rosa G., Caraglia M., New self-assembly nanoparticles and stealth liposomes for the delivery of zoledronic acid: a comparative study, Biotechnol. Adv., 2012; 30,302-9. doi: 10.1016/j.biotechadv.2011.06.018.

Mostaghaci, B., Loretz, B., Lehr, C.M., 2016. Calcium phosphate system for gene delivery: historical background and emerging opportunities. Curr. Pharm. Des. 22 (11), 1529–1533. https://doi.org/10.2174/1381612822666151210123859.

Obika, S., Yu W., Shimoyama A., Uneda T., Minami T., Miyashita K., Doi T., Imanishi T.,

Properties of cationic liposomes composed of cationic lipid YKS-220 having an ester linkage: adequate stability, high transfection efficiency, and low cytotoxicity, Biol. Pharm. Bull., 1999; 22(2):187-90.

Ochs, K., Kaina, B., 2000. Apoptosis induced by DNA damage O6-methylguanine is Bcl-2 and caspase-9/3 regulated and Fas/caspase-8 independent. Cancer Res. 60 (20), 5815–5824.

Pegg, A.E., 1990. Mammalian O6-alkylguanine-DNA alkyltransferase: regulation and importance in response to alkylating carcinogenic and therapeutic agents. Cancer Res. 50 (19), 6119–6129.

Perazzoli, G., Prados, J., Ortiz, R., Caba, O., Cabeza, L., Berdasco, M., Gónzalez, B., Melguizo, C., 2015. Temozolomide resistance in glioblastoma cell lines: implication of MGMT, MMR, P-glycoprotein and CD133 expression. PLOS ONE 10 (10), e0140131. https://doi.org/10.1371/journal.pone.0140131.

Porru, M., Zappavigna, S., Salzano, G., Luce, A., Stoppacciaro, A., Balestrieri, M.L., Artuso, S., Lusa, S., De Rosa, G., Leonetti, C., Caraglia, M., 2014. Medical treatment of orthotopic glioblastoma with transferrin-conjugated nanoparticles encapsulating zoledronic acid. Oncotarget 5, 10446–10459. https://doi.org/10.18632/oncotarget.2182.

Rädler, J.O., Koltover, I., Salditt, T., Safinya, C.R., 1997. Structure of DNA-cationic liposome complexes: DNA intercalation in multilamellar membranes in distinct interhelical packing regimes. Science 275 (5301), 810–814. https://doi.org/10.1126/science.275.5301.810.

Salzano, G., Marra, M., Porru, M., Zappavigna, S., Abbruzzese, A., La Rotonda, M.I., Leonetti, C., Caraglia, M., De Rosa, G., 2011. Self-assembly nanoparticles for the delivery of bisphosphonates into tumors. Int. J. Pharm. 403, 292. https://doi.org/10.1016/j.ijpharm.2010.10.046.

Salzano, G., Zappavigna, S., Luce, A., D'Onofrio, N., Balestrieri, M.L., Grimaldi, A., Lusa, S., Ingrosso, D., Artuso, S., Porru, M., Leonetti, C., Caraglia, M., De Rosa, G., 2016. Transferrin-targeted nanoparticles containing zoledronic acid as a potential tool to inhibit glioblastoma growth. J. Biomed. Nanotechnol. 12, 811–830.

Shi, F., Wasungu, L., Nomden, A., Stuart, M.C.A., Polushkin, E., Engberts, J.B., Hoekstra, D., 2002. Interference of poly(ethylene glycol)–lipid analogues with cationic-lipid-mediated delivery of oligonucleotides; role of lipid exchangeability and non-lamellar transitions. Biochem. J. 366, 333–341. https://doi.org/10.1042/BJ20020590.

Smisterová, J., Wagenaar, A., Stuart, M.C., Polushkin, E., ten Brinke, G., Hulst, R., Engberts, J.B., Hoekstra, D., 2001. Molecular shape of the cationic lipid controls the structure of cationic lipid/dioleylphosphatidylethanolamine-DNA complexes and the efficiency of gene delivery. J. Biol. Chem. 276 (50), 47615–47622. https://doi.org/10.1074/jbc.M106199200.

Stupp, R., Hegi, M.E., Mason, W.P., van den Bent, M.J., Taphoorn, M.J., Janzer, R.C., Ludwin, S.K., Allgeier, A., Fisher, B., Belanger, K., Hau, P., Brandes, A.A., Gijtenbeek, J., Marosi, C., Vecht, C.J., Mokhtari, K., Wesseling, P., Villa, S., Eisenhauer, E., Gorlia, T., Weller, M., Lacombe, D., Cairncross, J.G., Mirimanoff, R.O., European Organisation for Research and Treatment of Cancer Brain Tumour and Radiation Oncology Groups, National Cancer Institute of Canada Clinical Trials Group, 2009. Effects of radiotherapy with concomitant and adjuvant temozolomide versus radiotherapy alone on survival in glioblastoma in a randomised phase III study: 5-year analysis of the EORTC-NCIC trial. Lancet Oncol. 10 (5), 459–466. https://doi.org/10.1016/S1470-2045(09)70025-7.

Vuddanda, P.R., Rajamanickam, V.M., Yaspal, M., Singh, S., 2014. Investigations on agglomeration and haemocompatibility of vitamin E TPGS surface modified berberine chloride nanoparticles. Biomed. Res. Int. 2014, 951942 doi: 10.1155/2014/951942. doi: 10.1016/s0009-3084(99)00059-6.

Xiong, F., Mi, Z., Gu, N., 2011. Cationic liposomes as gene delivery systems: Transfection efficiency and new application. Pharmazie 66, 158–164.

Xu, C., Wang, J., 2015. Delivery systems for siRNA drug development in cancer therapy. Asian J. Pharm. Sci. 10 (1), 1–12. https://doi.org/10.1016/j.ajps.2014.08.011.

Xu, X., Li, Z., Zhao, X., Keen, L., Kong, X., Calcium phosphate nanoparticles-based systems for siRNA delivery, Regen. Biomater., 2016; 3(3):187-95. doi: 10.1093/rb/rbw010.

Xue, H.Y., Guo, P., Wen, C.W., Wong, H.L., 2015. Lipid-based nanocarriers for RNA delivery. Curr. Pharm. Des. 21, 3140–3147. https://doi.org/10.2174/1381612821666150531164540.